Journal of Power Sources 196 (2011) 652–658

Contents lists available at ScienceDirect

Journal of Power Sources

journal homepage: www.elsevier.com/locate/jpowsour

Analysis of in situ water transport in Nafion® by confocal micro-Raman spectroscopy

Yuichiro Tabuchi*, Rei Ito, Shohji Tsushima, Shuichiro Hirai

Research Center for Carbon Recycling and Energy, Tokyo Institute of Technology, 2-12-1 O-okayama, Meguro-Ku, Tokyo 152-8552, Japan

ARTICLE INFO

Article history:
Received 2 March 2010
Received in revised form 9 July 2010
Accepted 21 July 2010
Available online 30 July 2010

Keywords:
PEMFC
Water management
Nafion®
Raman spectroscopy
Water permeation

ABSTRACT

A proton exchange membrane fuel cell (PEMFC) is a promising alternative source of clean power for automotive applications, but its acceptance in such applications depends on reducing its costs and increasing its power density to achieve greater compactness. To meet these requirements, further improvements in cell performance are required. In particular, when the fuel cell is operating at high current density, the transport of water through the membrane has considerable impacts on the performance because of the large concentration gradient of water between the cathode and anode. Through-plane water permeation across the membrane is therefore a fundamental process in operational PEMFCs. Recently, resistance to water transport at the membrane–gas interface has been reported, and this is affected by the temperature and relative humidity. We investigated the distribution of water inside a proton exchange membrane during a water permeation test by using confocal micro-Raman spectroscopy with a fine spatial resolution (2–3 μm). In the presence of a water flux, the local water content is not necessarily in equilibrium with the water activity in the gas phase. Interfacial water-transport resistance due to the presence of a non-equilibrium membrane structure at the interface cannot be neglected.

1. Introduction

A proton exchange membrane fuel cell (PEMFC) is regarded as a promising alternative source of clean energy for automotive applications. Among the key challenges for acceptance of the PEMFC in automobiles are a reduction in its cost and an improvement in its power density for greater compactness. To solve these problems, further improvements in the fuel cell performance are required. Heat and water transport in the PEMFC are known to have considerable impacts on the performance of fuel cells operating at high current density. Because water is produced at the cathode and there is electro-osmotic drag between the anode and cathode, a large water-concentration gradient can build up between the electrodes of an operating PEMFC. Furthermore, a polymer electrolyte membrane (PEM) of a material such as Nafion® requires a certain degree of hydration to maintain its proton conductivity. To permit an electrochemical reaction to occur at the electrodes, the PEM needs to be capable of blocking the transfer of electrons and of reactants such as hydrogen and oxygen. Ideally, an electrolyte membrane for a PEMFC needs to be capable of transporting ions rapidly while blocking the passage of reactants. In addition to this, because of the large gradient in water concentration between the cathode and anode, water transport has to be sufficiently rapid to maintain an adequate degree of hydration of the membrane. Water management in the membrane is therefore of considerable importance in improving the performance of a PEMFC operating at high current density.

From the macroscopic point of view, the transport of water through the electrolyte membrane in a PEMFC has been described in terms of diffusion of water from the cathode to the anode and electro-osmotic drag between the anode and cathode as functions of the water content of the membrane [1–4]. The water-content curve is known to be function of the relative humidity (RH) [5]. Water is absorbed into the membrane, and strongly interacts with sulfonic acid groups in the membrane as a result of chemisorption at low water activity region. More water is absorbed into the membrane with weak interaction and structure change, called swelling at higher water activity region as a result of physical adsorption. In addition, resistance to transport of interfacial water in Nafion® membranes in the presence of a flux of water has been proposed [6–8]. It is considered that a large gradient in the concentration of water changes the surface morphology of the membrane and that a skin layer is formed on the membrane's surface. However, this fundamental mechanism has been considered only from the point of view of results for macroscopic permeation of water. A better fundamental understanding of the transport of water through the membrane is therefore needed.

From the microscopic point of view, the PEM combines a highly hydrophobic backbone and highly hydrophilic sulfonic acid functional groups. These sulfonic groups aggregate to form ionic clusters

* Corresponding author. Tel.: +81 3 5734 3554; fax: +81 3 5734 3554.
E-mail address: tabuchi.y.ac@m.titech.ac.jp (Y. Tabuchi).

0378-7753/$ – see front matter © 2010 Elsevier B.V. All rights reserved.
doi:10.1016/j.jpowsour.2010.07.078

through which water and proton are transported. The transport of proton and water is therefore significantly affected by the structure of the ionic clusters [9].

With this background, extensive diagnostic research has been performed in an attempt to achieve a fundamental understanding of water transport through PEMs. In microscopic analyses, the microstructure of the ionic clusters has been investigated by means of small-angle X-ray scattering and small-angle neutron scattering experiments. Because diffraction experiments on specific samples gave inadequate information, Gebel et al. performed diffraction studies on samples prepared over a wide range of polymer–solvent ratios and on samples prepared by using various solvents [10–12]. In addition to microscopic studies, analyses of macroscopic water permeation and diagnostic research on the distribution of water content in the thickness direction have been conducted. Although it has limited spatial resolution (10–20 μm) and limited applications to fluorinated sulfonic ion-exchange membranes such as Nafion®, the quantification of the water content by magnetic-resonance imaging (MRI) gave results that agreed well with those of a gravimetric method [13,14]. MRI therefore has considerable advantages in the quantification of the water-content distribution between the cathode and anode. MRI also allows quantitative determination of water transport in situ inside the membrane of an operating fuel cell. The neutron imaging technique (NRG) has also been used to quantify the water content of Nafion® membranes [15,16]. NRG has a high sensitivity to water inside the fuel cell, and it can be used to visualize and quantify the water distribution inside a PEMFC under in situ conditions. In particular, NRG has the great advantage that it is capable of visualizing the water distribution not only inside the membrane, but also in porous media made of carbon materials. It is therefore very helpful in achieving an understanding of the relationship between the water activity and the water content of a membrane. Confocal micro-Raman spectroscopy has also been used to analyze water-content distributions. This is a sensitive, noninvasive, and nondestructive technique that can be used to provide a direct measurement of the chemical contents of transparent films. The principal advantage of confocal micro-Raman spectroscopy is its fine spatial resolution (2–5 μm), which permits the analysis of the water-content distribution in thinner membrane than is possible by using MRI or NRG [17]. In addition, micro-Raman spectroscopy can distinguish between the water content and the methanol content of a membrane from their different modes of vibration [18,19].

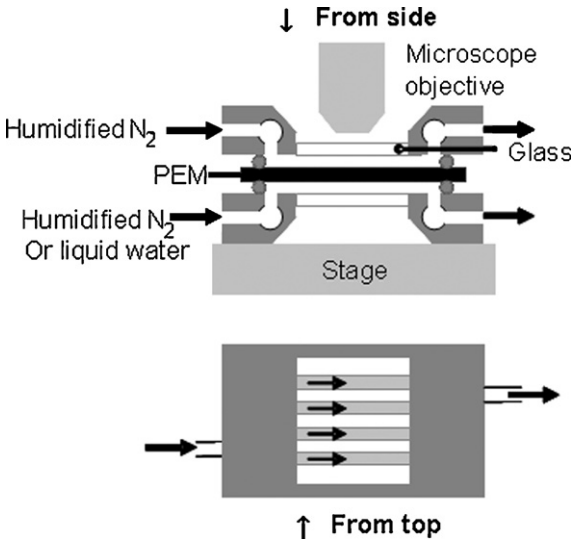

Fig. 1. Schematic of the microfluidic cell.

We used confocal micro-Raman spectroscopy to investigate the water-content profile in a Nafion® membrane in the presence of a steep gradient in water concentration, typical of the operating conditions of a PEMFC for automobile applications. A microfluidic cell was specially designed to permit the evaluation of the water-content distribution in situ under water permeation conditions. Initially, we confirmed the feasibility of analyzing the water content by means of confocal micro-Raman spectroscopy by comparison with the results of a gravimetric method. Secondly, dynamic water-content profiles were determined, and the existence of interfacial resistance to water transport is proposed. Finally, water-content profiles in membranes of various thicknesses were evaluated, and it was concluded that the interfacial water-transport resistance could be the result of a non-equilibrium change in the structure of the Nafion® membrane caused by the large water-concentration gradient.

2. Experimental

2.1. Materials

This study was carried out with different thickness of membranes; NRE 211 (25 μm), NRE 212 (50 μm), Nafion® 115 (125 μm), and Nafion® 1110 (250 μm) from DuPont (equivalent weight 1100 g equiv^{-1}), which are same type of polymer electrolyte membranes with different thickness. The samples were pretreated by a common procedure involving sequential treatment for 1 h in 3 wt% H_2O_2 solution, 1 h in boiled water, 1 h in 1 M aqueous H_2SO_4, 1 h in boiled water, and 24 h in pure water at room temperature.

2.2. Experimental cell and operating condition

A special microfluidic cell made of glass that is transparent to laser radiation was developed for the confocal micro-Raman spectroscopy studies; the cell is shown schematically in Fig. 1. The cell contained four straight channels on either side of the membrane and was equipped with an electric heater outside the gas channels to control the operating temperature. The Nafion® membrane was sandwiched inside the microfluidic cell to permit the introduction on opposite sides of the membrane of nitrogen gas with different levels of humidity. Fig. 2 shows the experimental apparatus. The microfluidic cell was placed on the stage in a microscope. The RH was controlled by passing the nitrogen gas through a series of bubblers. In the case where liquid water was used, this was introduced directly at a constant temperature by using a coolant pump. The laser was shone through the microscope, and the confocal point was controlled by minimizing the size of the laser spot on the surface of membrane at the inlet of gas flow. Table 1 shows the steady-state experimental conditions. Gas at the same level of humidity was introduced on both sides of the membrane to investigate the possibility of evaluating the water-content distribution by confocal micro-Raman spectroscopy. The RH was varied between 0 and 80%, and the equipment was kept at room temperature and ambient pressure. A flow of 10 L min^{-1} of nitrogen gas was maintained to minimize any distribution in RH in the flow direction and the depth direction of the gas channel. Table 2 shows

Table 1
Experimental conditions for steady-state studies.

Membrane	N 1110
Flow field	Rib/Channel = 0.5/1.5 mm, four straight channels
Active area	30 cm^2
Temperature	Room temperature (~30 °C)
Relative humidity	0, 30, 50, 65, or 80% or liquid water on both sides
Inlet pressure	Ambient pressure
Flow rate	10 L min^{-1}, nitrogen gas

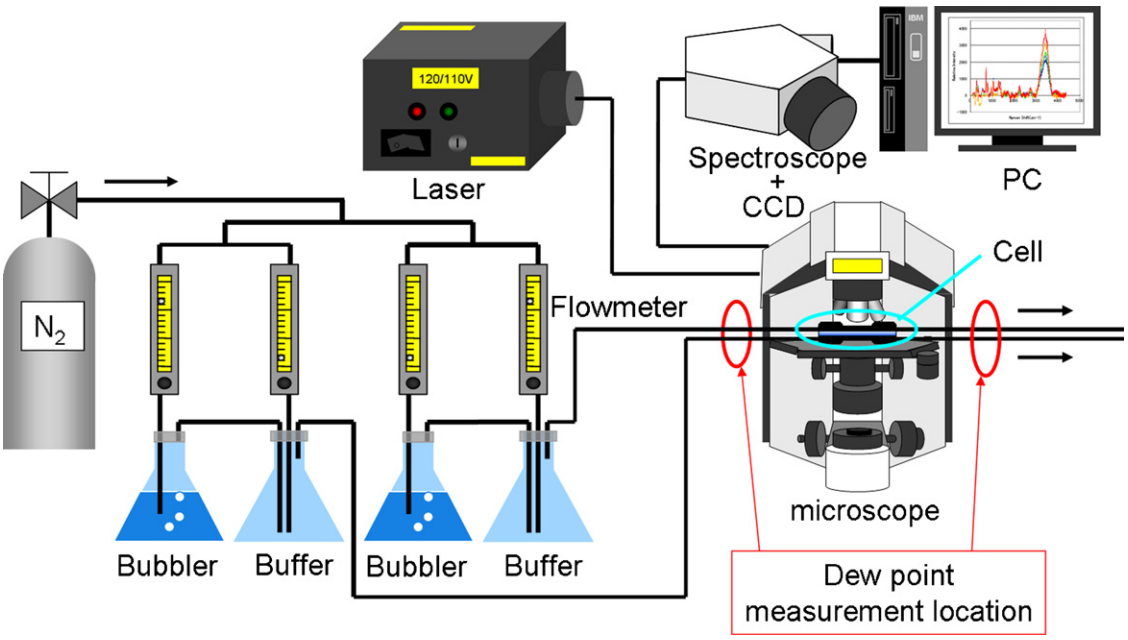

Fig. 2. Schematic of the experimental system.

the experimental condition for the water permeation study. Dry nitrogen gas of 10 L min^{-1} was introduced at the dry side, and humidified gas with different levels of humidity was introduced at 10 L min^{-1} on the opposite side of the membrane. The effect of the water-concentration gradient on the transport of water through the membrane was investigated by changing the RH at the wet side of membrane from 50 to 90% and to liquid water in the case of Nafion 1110. Furthermore, the effects of the water flux were investigated by changing the thickness of the membrane from 25 (NRE 211) to 250 μm (Nafion® 1110) with 0% RH on the dry side of the membrane and liquid water on the wet side. Finally, the effect of temperature was investigated in Nafion® 115 with dry gas on the dry side and liquid water on the wet side.

2.3. Raman spectroscopy measurements

Raman spectra were obtained by excitation with radiation of wavelength 532.0 nm from a Nd-YAG laser operating at about 20 mW. The spectra were recorded at room temperature by using a LABRAM 1B confocal Raman spectrometer (Jobin-Yvon S.A., Horiba, France) equipped with a charge-coupled device (CCD) detector cooled by means of a Peltier cooler. The spectrometer was coupled to the experimental cell described above by means of an Olympus microscope of 100 magnifications. The measurement technique offers the possibility of performing a depth scan through the Nafion® membrane to measure the concentration profiles of permeated water. The in-depth resolution of the objectives was about 2–3 μm, as determined by using a mechanical gauze (resolution 1 μm) and the volume of the confocal laser pinhole. The objective focused the laser beam into a measuring volume at the surface of the Nafion® membrane at the inlet of humidified gas under the channel, and the spot was then progressively displaced inside the polymer as far as the membrane surface on the opposite side. Because of large mass flow rate of 10 L min^{-1} and the measuring point at the inlet of humidified gas, relative humidity distribution in the gas channel can be negligible in water-content distribution by Raman spectroscopy in this system. The elastically (Rayleigh) and inelastically (Raman) scattered light was collected at each point in the direction of the membrane thickness by the objective, and was reflected to the edge filter by a system of mirrors. The Raman light, which was frequency shifted towards the laser light, passed through the filter whereas the Rayleigh light was almost all reflected. After spatial filtering of the Raman radiation, the scattered light was spectrally separated with an optical grid and detected by the Peltier-cooled CCD detector. The signals from the CCD detector were processed and displayed as Raman spectra by means of software (LabSpec version5.42.18).

Table 2
Experimental conditions in the presence of water flux.

Membrane	
(Effect of water activity)	N 1110
(Effect of water flux)	NRE 211, NRE 212, N 115, N 1110
(Effect of temperature)	N 115
Active area	30 cm^2
Flow field	Rib/Channel = 0.5/1.5 mm, four straight channels
Cell temperature	Room temperature or 70 °C
Relative humidity	0% (dry side) 50 or 90% or liquid water (wet side)
Inlet pressure	Ambient
Flow rate	10 L min^{-1}, nitrogen gas

3. Results and discussion

3.1. Steady-state conditions

Fig. 3 shows Raman spectra of Nafion® membrane under various conditions of RH with no water flux. The main characteristic bands were observed at 570 cm^{-1} [$\delta(CF_2)$], 730 cm^{-1} [$\nu_s(CF_2)$], 805 cm^{-1} [ν(C–S)], 970 cm^{-1} [ν_s(C–S)], 1060 cm^{-1} [$\nu_s(SO_3^-)$], 1210 cm^{-1} [$\nu_{as}(CF_2)$], 1300 and 1380 cm^{-1} [ν_s(C–C)], and 3000–4000 cm^{-1} [ν(OH)]. These peaks correlated well with results obtained by Gruger et al. [20]. In general, the Raman signal is proportional to the concentration ($I = kc$, where k is a material-dependent coefficient). In our case, as shown in Fig. 3, the only peak whose intensity increased with increasing RH was the OH vibration peak between 3000 and 4000 cm^{-1}. This change in the OH vibration peak suggested that the water content in the Nafion® membrane increased with increasing RH. Fig. 4 shows a comparison of the water-activity and water-content curves (a–λ property) with those obtained from a gravimetric method by Springer and coworkers [5]. Water content

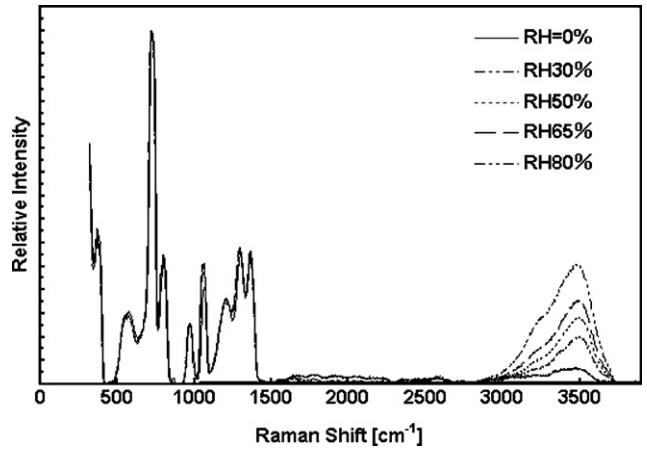

Fig. 3. Raman spectra of hydrated Nafion® 1110 under various conditions of RH.

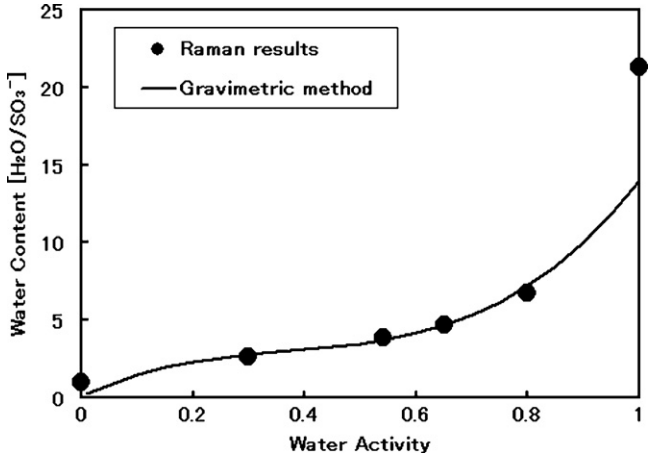

Fig. 4. Comparison of water contents measured by Raman spectroscopy with those obtained gravimetrically.

by Raman spectroscopy was evaluated from the relative intensity change from the calibration point of water activity of 0.5, which is assumed to be the same water content as gravimetric results, and then water-content profile in Fig. 4 was evaluated under various water activity conditions from the relative intensity change of the peak around 3500 cm^{-1} from the calibrated point. The quantified a–λ property from the Raman spectra correlated well with the gravimetric results. Furthermore, Fig. 5 shows the water-content

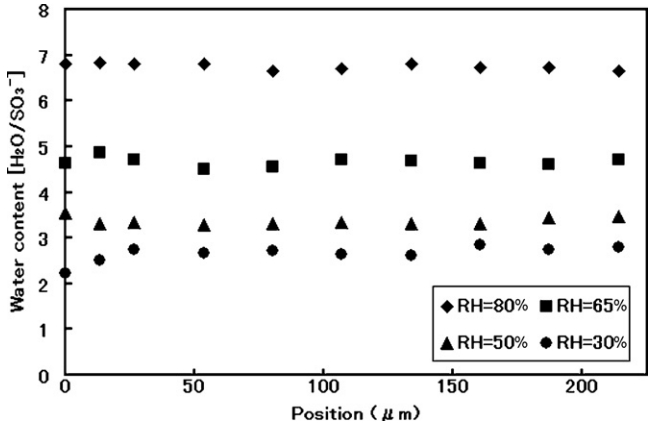

Fig. 5. Distribution of the water content through the membrane thickness under steady-state conditions.

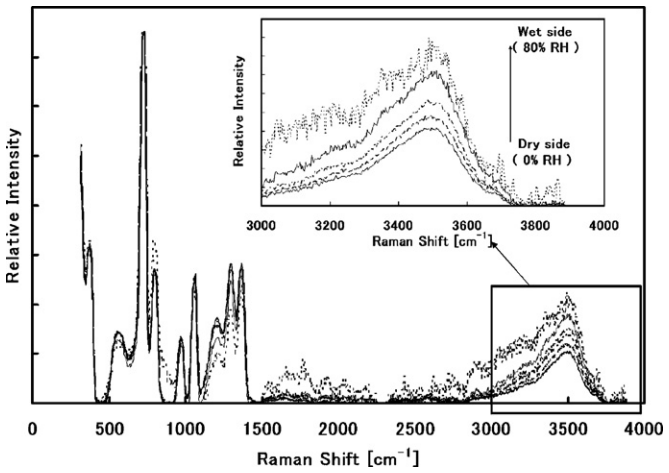

Fig. 6. Raman spectra in depth direction under water permeation condition of 0% RH at dry side and 80% RH at wet side.

distribution throughout the thickness of the membrane under various conditions of RH. Because there was no gradient in the water concentration, a uniform distribution of the water content was observed for each value of the RH. From these results, we confirmed that the water-concentration distribution can be measured quantitatively by means of confocal micro-Raman spectroscopy.

3.2. Water permeation conditions

Fig. 6 shows typical Raman spectra in depth direction under water permeation condition of 0% RH at dry side and 80% RH at wet side. The objective of microscope focused the laser beam into a measuring volume at the surface of the Nafion® membrane at the inlet of dry gas under the channel, and the spot was then progressively displaced inside the polymer as far as the membrane surface on the opposite side where relative humidity was controlled at 80%. Only OH vibration peak from 3000 to 4000 cm^{-1} was increased from dry side to wet side of the membrane. Water content at each position of the membrane was determined by water-content property shown in Fig. 4 and the relative intensity change of OH vibration peak around 3500 cm^{-1} in the presence of water flux whose peak was theoretically assigned to OH stretching vibration of H_2O molecule. Water-content distribution under the water permeation conditions in Table 2 was evaluated through this analytical method.

Fig. 7 shows the water-content distribution in the presence of a flux of water by the analytical method above described. Dry nitrogen gas was introduced over the dry side of the membrane, and

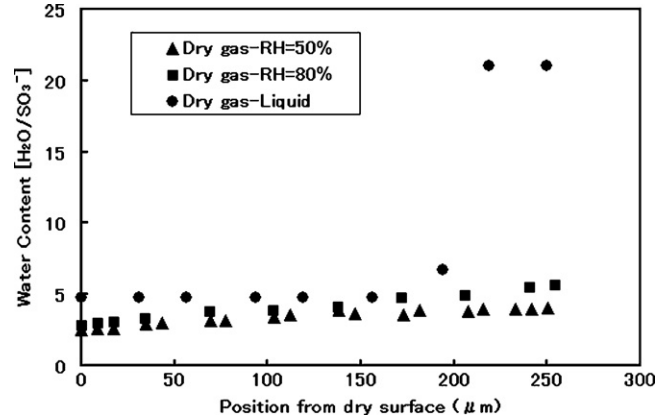

Fig. 7. Water-content distributions for various levels of RH at the wet side of a Nafion 1110 membrane.

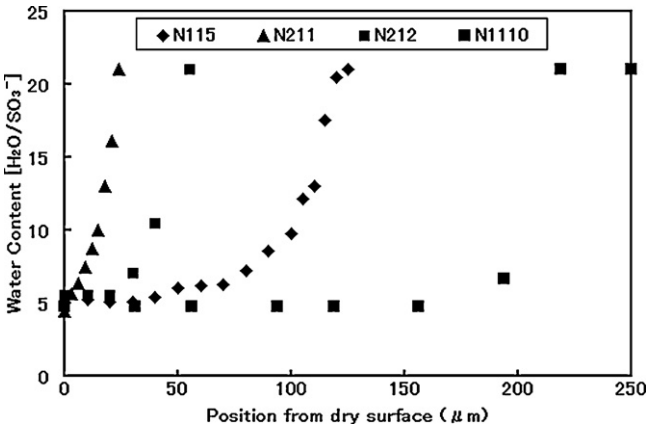

Fig. 8. Water-content distribution in case of different membrane thickness.

the RH on the wet side was kept 50 or 80%, or liquid water was present. As can be seen in Fig. 7, the water content on the wet side correlated reasonably well with the steady-state results, except in the case of 80% RH on the wet side. However, the water content on the dry side was not in equilibrium with the water activity on the dry side, and it increased with increasing water activity on the wet side of the membrane. This implies the existence of an interfacial resistance to water transport at the surface of the membrane. This could be caused by two factors: a difference in water activity near the membrane's surface from water activity in the gas channel as a result of the flux of water through the membrane, or a difference in the surface structure of membrane in comparison with that under steady-state conditions as a result of swelling. Both of these factors could occur with an increase in the water activity on the wet side of the membrane, as shown in Fig. 7. To distinguish between these possible factors, the effects of water flux were investigated by changing the thickness of the membrane, as shown in Fig. 8. The water contents on the dry sides of membranes with different thickness were identical to one another when the water-content gradient was the same. This suggests that the non-equilibrium water content at the dry side of the membrane is independent of the water flux. In other words, the water activity near the surface of the membrane was almost in equilibrium with the water activity in the gas channel as a result of the presence of a sufficient gas-flow rate. Fig. 9 shows the water-content distribution at 70 °C. Lower water content at the dry side was observed in comparison with that at room temperature. Furthermore, the water content increased with increasing temperature. This suggested that the water flux through the membrane increased as a result of an increase in the coefficient of diffusion of water in the membrane. However, the water flux did not affect the non-equilibrium water content on the dry side of the membrane at room temperature as shown in Fig. 8. So, it also suggested that water content at the surface of the dry side in the presence of water flux was not necessarily equilibrium with water activity at the gas channel due to the surface structure change caused by large water-content gradient through the membrane. In general, the elastic modulus of Nafion® decreases with increasing temperature and increasing RH. The swelling rate of Nafion® therefore increases with increasing temperature for the same water-concentration gradient. The lower non-equilibrium water content on the dry side could therefore be caused by a non-equilibrium structure of the surface of membrane, the presence of which is strongly related to the water-content gradient from the wet to the dry side.

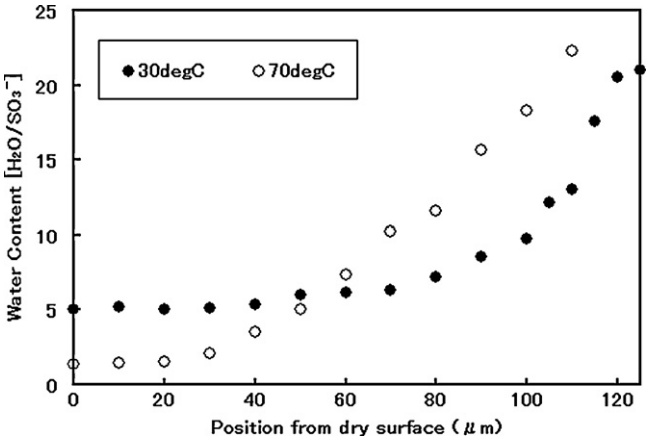

Fig. 9. Water-content distributions at various temperatures.

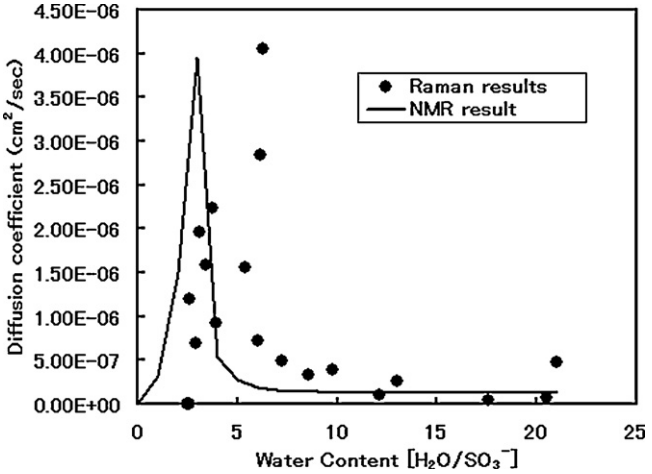

Fig. 10. Comparison of the water-diffusion coefficient measured by Raman spectroscopy with those obtained by an NMR study.

This non-equilibrium effect on water transport through the membrane was investigated to obtain a deeper fundamental understanding. Fig. 10 shows the relationship between the water content and the water diffusion coefficient at room temperature, as calculated from the water flux and the water-content gradient at each point from the Raman results by using the following equation:

$$D_{eff} = \frac{EW}{\rho M}\frac{\partial x}{\partial \lambda}J \tag{1}$$

where EW is the equivalent weight, ρ is the density of the membrane, and M is the molecular weight of water, λ is the water content, and J is the water flux. The calculated results agreed well to the other experimental results. This suggests that the operating water permeation conditions and the results of the quantitative analysis by Raman spectroscopy were reasonable, and that the water-concentration diffusion occurs by the same mechanism as that identified by other researchers [1,3]. Fig. 11 summarizes the contribution of interfacial water-transport resistance to the total water-transport resistance on the basis of the following three equations:

$$R_{diff} = \frac{\rho M}{EW}\frac{\lambda_{\mathrm{int},wet} - \lambda_{\mathrm{int},dry}}{J} \tag{2}$$

$$R_{\mathrm{int},wet} = \frac{\rho M}{EW}\frac{\lambda_{vap,wet} - \lambda_{\mathrm{int},wet}}{J} \tag{3}$$

$$R_{\mathrm{int},dry} = \frac{\rho M}{EW}\frac{\lambda_{\mathrm{int},dry} - \lambda_{vap,dry}}{J} \tag{4}$$

where R_{diff} is the internal water-transport resistance of the membrane, and R_{int} is the interfacial water-transport resistance. λ_{int} is

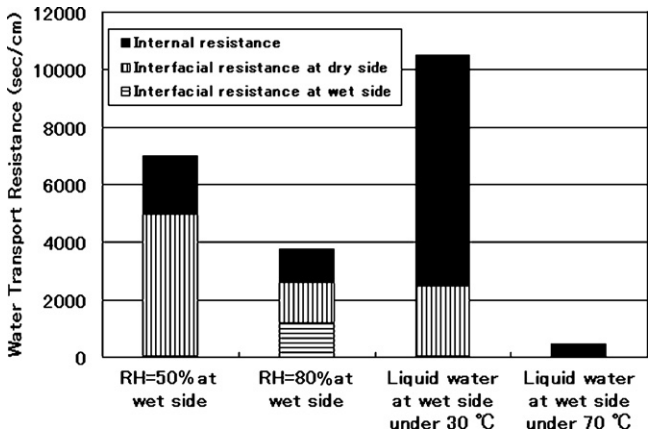

Fig. 11. The contribution of the interfacial and internal water-transport resistances to the total water-transport resistance of Nafion® 1110.

the water content at the interface of the membrane in the presence of water flux condition from micro-Raman spectroscopy, and λ_{vap} is water-content equilibrium with relative humidity at the gas channel in no water flux condition. So, R_{int} is defined as the water-transport resistance due to non-equilibrium water content at the surface of the membrane in the presence of water flux. The contribution of the non-equilibrium water content to the total water-transport resistance through the membrane was not negligible and it decreased with increasing RH at the wet side of the membrane. We believe that this tendency was caused by a change in the structure of Nafion® membrane as a result of the reduced elastic modulus of the membrane when a high RH was present at the wet side from the sensitivity results of operating temperature and membrane thickness to water-transport resistance through the membrane shown in Figs. 8 and 9. In the case where liquid water was present at the wet side, both the interfacial water-transport resistance at the dry side and the internal water-transport resistance increased in comparison with the case for water vapor. Because of the large water-concentration gradient from the wet side to the dry side, it is likely that greater rate of membrane swelling restricts structural relaxation of the membrane, resulting in a greater resistance to water-transport. At higher temperatures, however, the reduced elastic modulus caused a sufficient change in the membrane structure to produce a significant reduction in both the interfacial and internal water-transport resistance, even when liquid water was present at the wet side as shown in Fig. 9. Fig. 12 is a schematic showing the assumable mechanism of water-transport resistance in the presence of a large water-concentration gradient in the direction of the membrane thickness from Raman spectroscopy results in this study. As a result of the presence of different rates of swelling on the wet and dry sides of the membrane, the structure of the membrane at the interface is different from that where there is no water flux. Once a structural change has occurred, the equilibrium water content and water activity are changed, as are the water adsorption/desorption sites at the interface. As a result of the presence of resistance to water adsorption/desorption at the surface, the water flux decreases, and this causes the observed resistance to interfacial water transport. Furthermore, in the case of higher temperatures and higher levels of RH, lowering the elastic modulus relaxes the swelling-rate distribution in the membrane thickness. This results in sufficient relaxation of the membrane structure at the dry side of the membrane to lower the interfacial resistance to water transport. A large gradient in the water content in the membrane requires a large structural change between the wet side and the dry side, and a lower elastic modulus would be required to produce sufficient relaxation of the membrane structure at the dry side of the membrane.

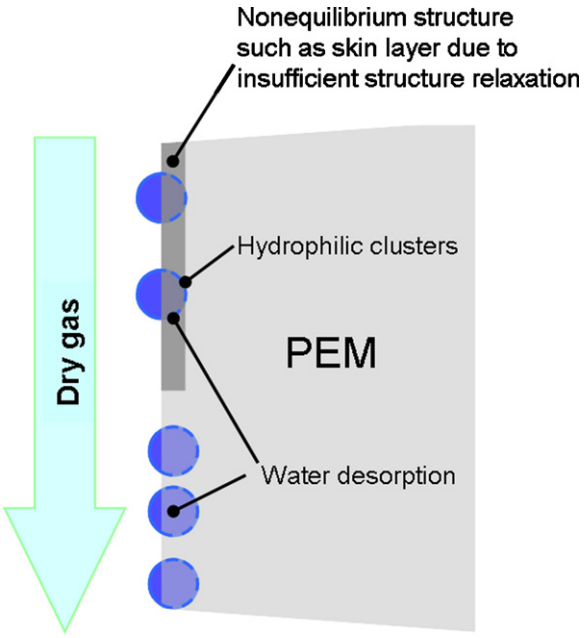

Fig. 12. Schematic representation of interfacial water transport through the membrane.

When considering the improvement of the performance of a fuel cell operating at a high current density, a large water-concentration gradient can readily occur as a result of the production of water at the cathode and the high water flux resulting from the electro-osmotic drag from anode to cathode. The use of a thin membrane is necessary to reduce losses caused by proton transport. However, the use of a thin membrane increases the water-concentration gradient between the cathode and anode. Back-diffusion of water is therefore necessary to maintain a sufficient degree of hydration of a membrane operating at a high current density, but interfacial water transport through the membrane has to be reduced to maintain proton conductivity at the anode and to reduce the quantity of effluent water at the cathode. Therefore, both the membrane thickness and its elastic modulus, in other words, the presence of sufficient structural relaxation of the membrane, are very important factors in the design of membranes for improved performance of fuel cells operating at high current density.

4. Conclusion

We have investigated the water-content distribution throughout the thickness of a Nafion® membrane by using confocal micro-Raman spectroscopy. Confocal micro-Raman spectroscopy allowed the measurement of the water content with a fine spatial resolution (2–3 μm). We found that a non-equilibrium water content at the gas–membrane interface occurred when a water flux was present. We also found that the non-equilibrium water content increased at lower temperatures and at higher levels of RH at the wet side of the membrane, and that it was insensitive to the water flux through the membrane. We suggest that the membrane structure was not in equilibrium with the water activity of the dry-side gas as a result of structural relaxation of the membrane. Furthermore, the effects on interfacial water transport through the membrane are not negligible, particularly in the case of the thinner membranes that are required to minimize proton transport losses in cells operating at high current density.

We conclude that not only concentration diffusion, but also the structure effect (in other words, the swelling effect) should be taken into account when considering water trans-

port through membranes operating at large water-concentration gradients.

Acknowledgements

We gratefully acknowledge financial support for this work provided by the Nissan Motor Co. Ltd. The authors are grateful to Mr. K. Aotani, Dr. N. Kubo, and Dr. K. Shinohara of the Nissan Motor Co. Ltd. for fruitful discussions regarding water transport through membranes and the performance of the PEMFC.

References

[1] T.E. Springer, T.A. Zawodzinski, S. Gottesfeld, J. Electrochem. Soc. 138 (1991) 2334.
[2] T.A. Zawodzinski, M. Neeman, L.O. Sillerud, S. Gottesfeld, J. Phys. Chem. 95 (1991) 6040.
[3] S. Motupally, A.J. Becker, J.W. Weidner, J. Electrochem. Soc. 147 (2000) 3171.
[4] T.A. Zawodzinski, J. Davey, J. Valerio, S. Gottesfeld, Electrochim. Acta 40 (1995) 297.
[5] T.A. Zawodzinski, C. Derouin, S. Rodzinski, R.J. Sherman, V.T. Smith, T.E. Springer, S. Gottesfeld, J. Electrochem. Soc. 140 (1993) 1041.
[6] P.W. Majsztrik, M.B. Satterfield, A.B. Bocarsly, J.B. Benzinger, J. Membr. Sci. 301 (2007) 93.
[7] K. Aotani, S. Miyazaki, N. Kubo, M. Katsuta, ECS Trans. 16 (2008) 341.
[8] C. Monroe, T. Romero, W. Merida, M. Eikerling, J. Membr. Sci. 324 (2008) 1.
[9] K.D. Kreuer, S.J. Paddison, E. Spohr, M. Schuster, Chem. Rev. 104 (2004) 4637.
[10] G. Gebel, P. Aldebert, M. Pineri, Polymer 34 (1993) 333.
[11] G. Gebel, J. Lambard, Macromolecules 30 (1997) 7914.
[12] G. Gebel, Polymer 41 (2000) 5829.
[13] S. Tsushima, T. Nanjo, K. Nishida, S. Hirai, ECS Trans. 1 (2006) 199.
[14] S. Tsushima, K. Teranishi, S. Hirai, Electrochem. Solid State Lett. 7 (2004) A269.
[15] P. Boillat, G.G. Scherer, A. Wokaum, G. Frei, E.H. Lehmann, Electrochem. Commun. 10 (2008) 1311.
[16] D.J. Ludlow, G.M. Calebrese, S.H. Yu, C.S. Dannehy, D.L. Jacobson, D.S. Hussey, M. Arif, M.K. Jensen, G.A. Eisman, J. Power Sources 162 (2006) 271.
[17] H. Matic, A. Lundblad, G. Lindbergh, P. Jacobsson, Electrochem. Solid State Lett. 8 (2005) A5.
[18] P. Scharfer, W. Schabel, M. Kind, J. Membr. Sci. 303 (2007) 37.
[19] S. Deabate, R. Fatnassi, P. Sistat, P. Huguet, J. Power Sources 176 (2008) 39.
[20] A. Gruger, A. Régis, T. Schmatko, P. Colomban, Vib. Spectrosc. 26 (2001) 215.